Design and test of a double compression seeder for pre-sowing and seed furrow of wheat in wide-seedling belts

Xun He[1], Run Zhang[1], Jingfeng Zhang[1], Yinghao Zhu[1], Wanzhang Wang[1*], Hongmei Zhang[1]
(1. *College of Mechanical and Electrical Engineering, Henan Agricultural University, Zhengzhou 450002, China*)

Abstract: To solve the problem of poor sowing quality due to loose soil in wheat seedbed after land preparation in the Huang-Huaihai region of China, a double compression seeder for pre-sowing and seed furrow of wheat in wide-seedling belts was designed. The machine sowing operation was divided into two processes: pre-sowing compression and seed ditch compression, pre-sowing compression was carried out homogenization of the pre-sowing seed bed that the tractor wheel has crushed, and the seed ditch compression compresses the seeds and soil in the seed ditch, so that the seeds were embedded in the seed ditch soil. By analyzing the kinematics of the pre-planting compression device and the spiral blade in the process of soil levelling and compression, the structure of the equal-difference variable-diameter equal-pitch spiral conveying winch was designed, and the key parameters of the drum spiral blade were determined, and then the height of the spiral blades, the rutting distance and the speed of the compression roller were taken as the test factors, and the soil flatness was used as the index to carry out the discrete element simulation test. The simulation results show that when the spiral blade was 4.85 cm, the rut distance was 37.4 cm, and the rotation speed was 327.16 r/min, the optimal land flatness was 0.18. Finally, field experiments were carried out on the seeder, and the results showed that: the soil bulk density after operation was 22.7% greater than that before sowing ($p < 0.01$), and the soil flatness was 1.9 cm, which was consistent with the simulated results. The use of pre-sowing compression and seed furrow compression methods improved the soil environment of the seed bed, increased the uniformity of the seeding depth, and promoted the root growth of wheat. This study provides equipment support and technical reference for agricultural production in wheat-corn rotation areas in the Huang-Huaihai region of China.
Keywords: wheat, seeding quality, pre-sowing compression, seed furrow compression, field experiment
DOI: 10.25165/j.ijabe.20241704.8369

Citation: He X, Zhang R, Zhang J F, Zhu Y H, Wang W Z, Zhang H M. Design and test of a double compression seeder for pre-sowing and seed furrow of wheat in wide-seedling belts. Int J Agric & Biol Eng, 2024; 17(4): 136–145.

1 Introduction

As the main production area of winter wheat in China, the Huang-Huaihai region, wheat pre-sowing preparation relies mostly on the rotary tillage method, the quality of preparation is poor, the soil void ratio is large, and the loss of entropy all result in poor quality of wheat sowing, and under the tractor used for sowing operations, soil crushing under the wheels will leave ruts, affecting the sowing depth and the control thereof[1-3]. The compound operation wheat seeder with the compression mechanism can build a high-quality seed bed soil structure, which can help sow wheat seeds in the predetermined soil position at a suitable depth, forming a reasonable row width, stable sowing depth, and suitable soil firmness, providing a good environment and conditions for seed germination and seedling growth[4-6].

Compression is a key measure to establish a quality seed bed in wheat sowing, which can increase the soil density in the seed belt and create a germination, emergence and growth environment for seeds with suitable soil density[7-9]. Wheat sowing compression is mainly divided into pre-sowing compression and post-sowing compression, pre-sowing compression is the compression before sowing after land preparation and post-sowing compression is the compression after sowing, both of which affect the quality of sowing operations[10]. Studies have shown that when the sowing depth is large, the soil in the cultivated layer of the seed belt cannot be compacted by increasing the counterweight of the press roller alone, or the top soil is over-compacted when the desired level of compaction is reached. When the surface soil is over-compacted, the soil capillary water rises, causing moisture loss and difficulty in precipitation infiltration, increasing surface runoff, and reducing the source of moisture to the soil; at the same time, if the mechanical resistance of the surface soil is larger than the emergence pressure of the seedlings, the seedlings cannot emerge from the soil[11-13].

Bronick et al.[14] found that the structure of a high-quality seedbed can be divided into three layers, which are the sub-soil, the top soil, and the soil surface mulch such as clods and stubble; the sub-soil should be compacted to facilitate moisture lifting; the top soil is loose and compacted to facilitate air and heat supply to the seed. Liu et al.[15] designed and determined the parameters of the crushed soil press roller installed after the deep loosening shovel and before the furrow opener on the seeder levelled the seed bed during seeding; the pre-sowing press roller of the double compression seeder was designed by Wei et al.[16] for wheat wide-seedling belt pre-sowing and post-sowing to realize the destruction of soil clods and compacted soil to meet the agronomic

Received date: 2023-06-06 **Accepted date:** 2024-05-07
Biographies: Xun He, PhD, Associate Professor, research interest: biomass harvesting and processing technology, Email: hexun@henau.edu.cn; **Run Zhang**, MS, research interest: modern agricultural equipment design, Email: runzhang2022@163.com; **Jingfeng Zhang**, MS, research interest: modern agricultural equipment design, Email：18317832610@163.com; **Yinghao Zhu**, PhD, Lecturer, research interest: design and measurement and control of modern agricultural equipment, Email: zyhzyh@henau.edu.cn; **Hongmei Zhang**, PhD, Professor, research interest: intelligent agricultural equipment and agricultural product detection technology, Email: zhanghongmei0905@henau.edu.cn.
***Corresponding author: Wanzhang Wang**, PhD, Professor, research interest: agricultural engineering and equipment. No.63, Nongye Road, Jinshui District, Zhengzhou 450002, China. Tel: +86-371-63558040, Email: wangwz@henau.edu.cn.

requirements of pre-sowing preparation. In post-sowing compression, Zhao et al.[17] designed a multifunctional integrated seeding opener integrating furrow opening, soil return and compression, after opening the seed furrow, the seeds fall to the bottom of the furrow, the wet soil returns to the furrow, the press roller compresses the seed furrow, and the seeds are forced into close contact with the soil. Jia et al.[18] designed a synchronous seed furrow compaction device for furrow opening, which can realize compaction and reshaping of the original seed furrow and improve the consistency of the seed sowing depth; Xi et al.[19] designed a groove press wheel to press out a concave seed groove after rototilling the soil and then sow the seeds, which has less soil return and a stable shape of the seed groove, which is conducive to uniform sowing of wheat. At present, the research on post-sowing compression is mainly focused on compression after sowing and mulching, but there is less research on compression after wheat seeds fall into the seed furrow during sowing.

To this end, in view of the technical problems of rutting and seed trench compression left by tractor driving operation, a double compression seeder for pre-sowing and seed furrow of wheat in wide-seedling belts was designed, and a planting method involving pre-sowing compression and seed trench compression was proposed: this solves the problems of rutting and pre-sowing soil looseness left by tractor driving operation while pre-sowing compression, and seed trench compression suppresses the seeds after they fall into the seed trench. The seed furrow compression is undertaken after the seeds are dropped into the seed furrow, so that the seeds are in close contact with the soil, thus establishing a loose seed bed environment for the seeds and improve the quality of the wheat-sowing operation. It provides equipment support and technical reference for agricultural production in the wheat-corn rotation in the Huang-Huaihai region of China.

2 Whole machine structure and working principle

2.1 Whole machine structure

According to the requirements of wheat-corn crop rotation, the overall structure of a double compression seeder for pre-sowing and seed furrow of wheat in wide-seedling belts is shown in Figure 1.

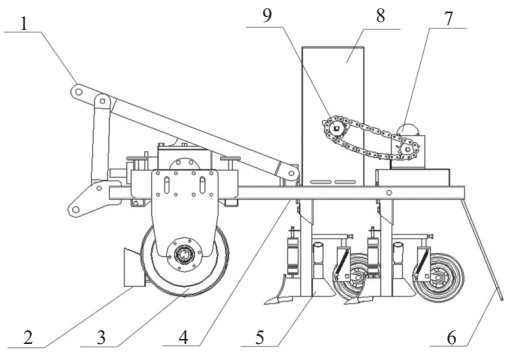

1. Three-point hitch 2. Soil separators 3. Pre-sowing leveling and compressing device 4. Frame 5. Seed furrow compression seeding monomer 6. mulcher 7. Electrically driven seeding device 8. Seed box 9. Seed dispenser

Figure 1 Organization structure diagram

The main parameters are listed in Table 1. The pre-planting compression device is installed in the front of the machine; the seed box is fixed in the middle of the frame, the outer groove wheel type seed rower is installed under the seed box, the electric drive seeding device is installed on the pedal behind the seed box; the seed trench compression seeding unit is fixed under the frame, arranged in two rows, the depth of trenching is adjustable; the mulcher is installed behind the frame, the height and rotation angle are adjustable.

Table 1 Main parameters of the seeder

Parameters	Values
Dimensions/cm	200×230×120
Working width/m	2.4
Machine weight/kg	590
Matched power/kW	60-90
Hook mode	three-point hitch
Number of seeding rows	12
Sowing depth/cm	2-5
Subsoiling depth/cm	8+4+8+4+8+28
Seedling band width/cm	32
Type of seed metering device	outer groove-wheel

2.2 Working principle

During operation, the tractor pulls the seeder, the compression device fixed in the front of the seeder enters the soil, the spiral blade is powered by the tractor power take-off (PTO) shaft to rotate, pushing the scraped part of the soil to the initial end of the left and right spiral, respectively: the spiral blade pushes the soil on the surface of the middle seeding row to the ruts on the left and right to achieve the effect of levelling the land; the compression drum relies on the whole machine in the process of rotation to In the process of rotating, the compression roller relies on the self-weight of the machine to compact the soil of the seed bed before sowing.

When sowing, the electrically driven seeding device adopts a high-precision positioning module to measure the real-time operating speed of the seeder, control the motor speed according to the speed and adjust the motor speed in real time to control the rotation speed of the seeding outer groove wheel seed rower. The seeds are discharged from the seed rower and fall into the seed furrow through the seed tube. The press roller directly compresses the seed furrow and the seeds, compacting the seeds into the soil. Finally, the mulcher pushes the soil outside the seed trench into the seed trench to cover the seeds and complete the sowing operation.

3 Key component design

3.1 Design of pre-planting compression device

The soil in the wheat seed bed in the Huang-Huaihai region was loose after preparation, with relatively large soil pores and rapid water transpiration. After the tractor enters the field, the rutting produced reduces the consistency of the sowing depth of the seeding operation. Therefore, a pre-sowing compression device was designed, whose structure is shown in Figure 2, with the purpose of suppressing the loose pre-sowing soil and levelling the land pressed by the tractor wheels to create a good bed environment for the seeds.

The compression device is mainly composed of adjusting hand wheel, compression device frame, drum spiral blade, conical soil divider, gearbox, compression drum and other parts. The spiral blades on the left and right sides have opposite spiral lift angles. By adjusting the height of the roller through the hand wheel, the compression intensity can be adjusted so that the seeder can meet the effect of filling ruts and suppressing before sowing when working on the land with different looseness.

3.1.1 Design of spiral blade

The depth and width of the rut are the main factors in determining the amount of soil required. The amount of soil pushed by the spiral blade and conical divider should be theoretically the

same as the amount of soil previously filling the rut. Figure 3 shows a schematic representation of a pre-sowing compression device for tractor-mounted operation; in the present work an commonly used model LX1300 tractor (external dimensions 475 cm×218 cm×294 cm, rear wheel tyre width 4 cm, diameter 76.2 cm, minimum mass 2394 kg, minimum use specific mass ≥ 38 kg/kW, and PTO shaft speed is 540 r/min) was used. To prevent soil from being transported outside the rut, the width of the winch is slightly less than the width of the outer edge of the rut. The rut width b = 40 cm, L_a = 40 cm. The conical soil divider pushes the soil to the initial end of the winch, and the situation whereby the middle part of the conveying winch has more soil and the two sides have less soil may arise. To make the soil distribution uniform, a screw conveying strand of equal pitch with equal variation in diameter was adopted.

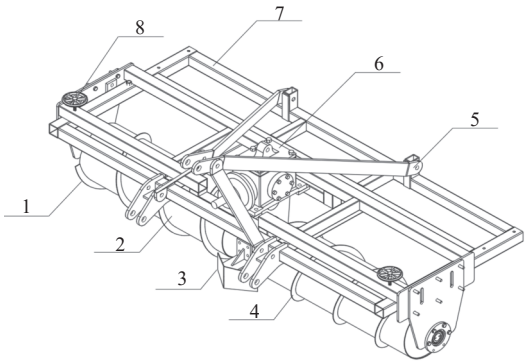

1. Terminate the end auger blades 2.Rotary burying roll 3. Beginning end auger blades 4. Conical separator 5. Suspension racks 6. Gearbox 7. Compression device rack 8. Adjust the handwheel

Figure 2 Structure diagram of compression device

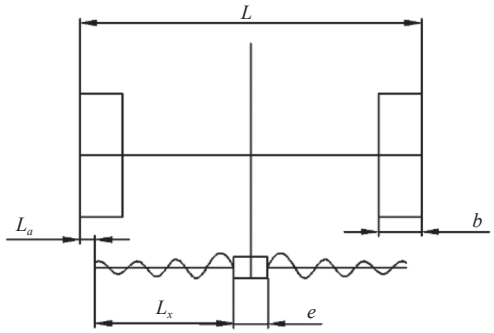

Note: L is the width of the tractor, cm; b is the width of the rut, cm; e is the width of the conical separator, cm; L_x is the length of the spiral, cm; L_a is the distance between the spiral blade and the outermost end of the rut, cm.

Figure 3 Schematic diagram of pre-sowing compressing device working with tractor

The compression device compresses and levels the soil at the same time, and if changes in soil firmness are not considered, the volume of soil before and after screw conveying remains the same. The amount of soil required to fill in the tractor ruts in the seeding operation (one side) can be calculated according to Equation (1)[20].

$$\begin{cases} Z = \left[\dfrac{3W}{(3-n_1)Kb\sqrt{D_0}}\right]^{\frac{2}{2n_1+1}} \\ d = b(Z-d)/f \\ f = (L-2b)/2 \end{cases} \quad (1)$$

where, Z is the rut depth, cm; W is the wheel load, daN; According to the minimum use mass of the vehicle to take W = 598.5 daN; n_1, K are the soil pressure characteristics parameters, for loose soil n_1 = 1.03, K = 0.169 daN/cm[20]; D_0 is the tractor wheel diameter, cm; The ground filled in at the rut is consistent with the ground height of the soil conveyed by the spiral blades. d represents the soil conveying depth, cm; f is the soil conveying width (single side), cm. According to the Equation (1), f=69 cm, d=2.2 cm, Z=6 cm. Because of the efficiency of the conveying device, the height of the screw blade should be greater than the soil conveying depth, and the actual screw blade into the soil depth is less than 9 cm, the height range of the screw blade is 9 cm≥h_0≥3 cm.

$$q = 3600(Z-d)\cdot b\cdot v_m\cdot\rho \quad (2)$$

where, q is the amount of soil required for rut filling, t/h; v_m was taken as medium speed of the seeder[21], m/s; v_m=1.67 m/s; ρ denotes the volume of soil contacted during the operation of the pre-sowing compression device, t/m^3; the value of 1.2 t/m^3[22] was taken as q=109.66 t/h. At the termination end of the screw conveying winch, the parameter[23-25] is selected according to the operating requirements, and its conveying volume is:

$$Q = 3600F_1\cdot\lambda\cdot v_1\cdot\varepsilon \quad (3)$$

$$F_1 = (D_1^2 - d_0^2)\cdot\psi\cdot\pi/4 \quad (4)$$

where, Q is the conveying volume at the end of the screw conveyor, t/h; D_1 is the diameter of the screw blade at the end, cm; F_1 is the cross-sectional area of the material layer in the trough, cm^2; λ stands for the mass of the material unit volume, t/m^3; λ is 1.2 t/m^3; ε is the spiral inclination conveying coefficient, the value of which is 1; d_0 is the shaft diameter of the compression roller, cm (this exerts a significant influence on the compression effect, its value should be less than the difference between the height of the frame and the height of the blade, namely d_0≤33 cm, according to the actual production situation, the value set to 30 cm herein; ψ is the material filling factor, the value is 0.3. The material in the tank axial movement speed $v_1 = S\cdot n/60$. v_1 is the axial movement speed, m/s; n is the spiral speed, r/min; S is the pitch, cm; PTO shaft speed is 540 r/min, transmission ratio is 15:24, so a value of 337.5 r/min was taken as the maximum herein. Under normal circumstances, the pitch S can be calculated by the following equation:

$$S = K_1\cdot D_2 \quad (5)$$

where, K_1 is the ratio coefficient of spiral diameter and spiral pitch, the pitch of standard conveyor is generally 0.8 < K_1 < 1.0; K_1≤0.8 when conveying materials with poor fluidity or in an inclined arrangement. D_2 is the starting end spiral blade diameter, cm. Soil is typically a poor-fluidity material, so to avoid soil plugging, S should be greater than or equal to twice the maximum side length of the soil block required to maintain the required rate of soil crushing; the maximum length of soil block in tilled land is 5 cm, at the same time, the pitch should be less than or equal to the diameter of the blade, namely 10 cm≤S≤38 cm (here S=38 cm). The conveying volume Q at the terminating end should be greater than the amount of soil required for rut filling q, thus D_1> d_0+2(Z-d)，and the sum of calculations D_1 > 37.6 cm, so here D_1 = 38 cm. This is substituted into Equation (2) to obtain Q = 89.65 t/h.

The conveying volume Q_0, t/h at the beginning of the screw includes not only the conveying volume of the rut, but also the conveying volume Q_1, t/h pushed by the conical soil divider, as given by

$$Q_1 = 3600e\cdot d\cdot v_m\cdot\lambda/2 \quad (6)$$

The value of the conical soil divider width e is 30 cm, and the calculated Q_1 = 23.80 t/h, then Q_0 =Q+Q_1 =113.45 t/h. Substituting Q_0 into Equation (2) yields the diameter of the starting spiral blade D_2=39.1 cm (nominally 40 cm). In summary, the pre-sowing compression device drum diameter is 30 cm, the starting end spiral blade diameter D_2≥40 cm, the ending end spiral blade diameter D_1≥38 cm, and the pitch S≥32 cm.

3.1.2 Spiral blade motion analysis

To select the best structure and position parameters of the compression screed roller under the optimal land levelling, a motion analysis of the spiral blade is conducted to calculate whether the required rotational speed meets the realistic requirements. When the compression roller is working, the spiral blade is a synthetic motion in the form of rotation and advancement with the roller, and its motion trajectory is that of a pendulum (Figure 4).

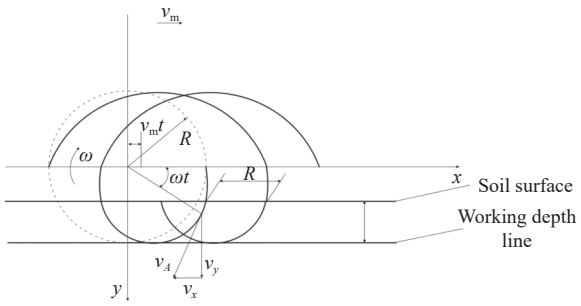

Note: R is the rotation diameter at the end of the spiral blade, cm; ω is the angular velocity of the drum rotation, rad/s; v_m is the forward speed of the seeder, m/s; t is the time, s; v_A is the tangential velocity at point A, m/s; v_x and v_y are the horizontal and vertical velocities of v_A, m/s.

Figure 4 Spiral motion track of pre sowing pressing device

Let the center of rotation of the drum as the coordinate origin, x-axis positive direction and the drum forward direction, y-axis direction vertically downwards, the initial phase of the blade end point is located in front of the horizontal position and coincide with the positive direction of the x-axis, then the spiral blade end point equation of motion is

$$x = R\cos\omega t + v_m t \tag{7}$$

$$y = R\sin\omega t \tag{8}$$

where, R is the rotational diameter of the spiral blade end point, cm; ω is the angular velocity of drum rotation, rad/s; v_m is the forward speed of the seeder, m/s; t is the time, s;

The partial velocity of the end point of the spiral blade in the direction of the x and y-axes is

$$v_x = \mathrm{d}x/\mathrm{d}t = v_m - R\omega\sin\omega t \tag{9}$$

$$v_y = \mathrm{d}r/\mathrm{d}t = R\omega\cos\omega t \tag{10}$$

The absolute velocity v at the end point of the spiral blade is

$$v = \sqrt{v_m^2 + R^2\omega^2 - 2v_m R\omega\sin\omega t} \tag{11}$$

where, $R\omega = v_p$ is the circumferential linear velocity of the end point of the spiral blade, m/s; so that $\lambda_1 = v_p/v_m = R\omega/v_m$, λ_1 is called the rotational speed ratio, the size of λ_1 has an important influence on the trajectory of the spiral blade movement and the working condition of the compression and levelling roller, leading to:

$$v_x = v_m - R\omega\sin\omega t = v_m(1 - \lambda_1\sin\omega t) \tag{12}$$

To meet the design requirements, v_x should be less than 0, then λ_1 should be greater than 1. When λ_1 < 1, that is, v_p < v_m, then no matter what position the spiral blade movement must be to ensure that v_x > 0, this will lead to the spiral blade being unable to cut backwards into the soil: the blade end point is pushed forwards into the soil, so that the compression device cannot work properly. If λ_1 > 1, when the spiral blade rotates to a certain position, there will be v_x < 0, the spiral blade can cut soil backwards. As long as the blade in the beginning of cutting soil v_x < 0, the movement trajectory of the cutting part of the blade in the whole process of cutting soil at each point is that of a residual pendulum, and its circumferential line speed v_p should be greater than the forward speed of the drum v_m. When λ_1 > 1, that is

$$n \geq \frac{v_m}{\pi D_2}\times 60 \tag{13}$$

The operating speed of the seeder v_m = 1.67 m/s, so the angular velocity of the roller should be greater than 88 r/min. The roller speed is 337.5 r/min, which meets the minimum-value requirement. In actual production, the screw conveyor when the conveying volume Q is certain, the screw conveying speed n should be within a certain range, and the maximum angular velocity $n_{\max}$ is

$$n_{\max} = 60A_0/\sqrt{D_2} \tag{14}$$

where, A_0 is an integrated coefficient (set to 15), so, for this design n≤1500 r/min, tractor PTO shaft speed of 540 r/min, giving n = 337.5 r/min to meet the maximum requirements, so the speed of the drum in this design meets requirements[23].

3.2 Seed furrow compression seeding monomer design

3.2.1 Overall structure and working principle

The seed furrow compression seeding unit mainly consists of a furrow opener, baffle plate, seed tube, seed furrow compression device, and so on. The core-share opener demonstrates a simple structure, strong soil entry capacity, and wide-seedling furrow, which can complete the furrowing operation in the land where the land preparation is not particularly good[26,27] therefore, the core-share furrow opener is used. The baffle reduces the amount of soil return in the seed furrow and prevents seed splashing.

The structure of the seed furrow compression device is shown in Figure 5, and the main structural parameters are listed in Table 2: the furrow opener is fixed on the beam, and the fixed frame is bolted to the beam, and its height is adjustable. The tension spring is connected to the fixed frame through the connecting bolt; the connecting plate is hinged to the fixed frame in the middle and connected to the press roller at the other end. The tension spring exerts downward pressure on the press roller by lever action to achieve compression of the seed furrow. The fixed frame has a sliding hole slot, and the spring end of the connecting rod is limited to the range of rotation allowed by the slot, which limits the floating lowest and highest points of the press roller, and the compression strength is adjustable (by changing the spring tension).

The effect of seed trench compression is shown in Figure 6. After the seed guide tube introduces the seeds into the seed trench of about 8 cm in width, the press roller of the seed trench compression device compresses the seeds and sets the seeds in the soil, while compacting the soil in the seed trench. Finally, under the action of the mulcher, the loose soil covers the seeds.

3.2.2 Design and parameter selection of a seed trench compression device

The profiling structure of the seed trench compression device is shown in Figure 7. L_{AC} is the length of the connecting plate, point B

is the hinge point between the connecting plate and the fixed frame, point D is the fixed position of the connecting bolt, γ is the traction angle (in service), (°); γ_1 is the lower profiling angle, (°); and $\gamma+\gamma_2$ is the upper profiling angle,(°).

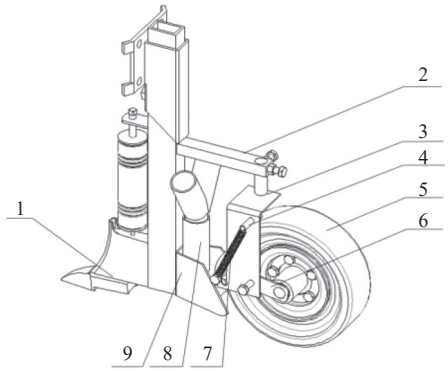

1.Opener 2.Beam 3.Fixed frame 4.Connecting bolt 5.Wheel of repression 6.Connecting plate 7.Extension spring 8.Seed dropping tube 9.Baffle

Figure 5 Diagram of seedling pressure seeding single

Table 2 Main parameters of the seeding monomer

Parameters	Value/cm
Trenching depth	3-5
Trench width	8
Upper profiling	5.14
Lower profiling	4
Diameter of the pressure wheel	23
Width of the pressure wheel	7

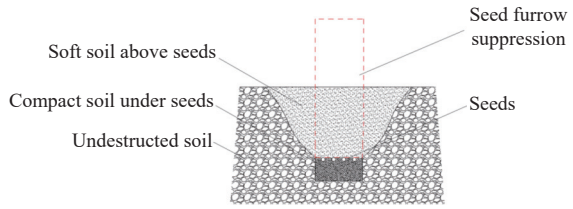

Figure 6 Schematic diagram of seed ditch suppression effect

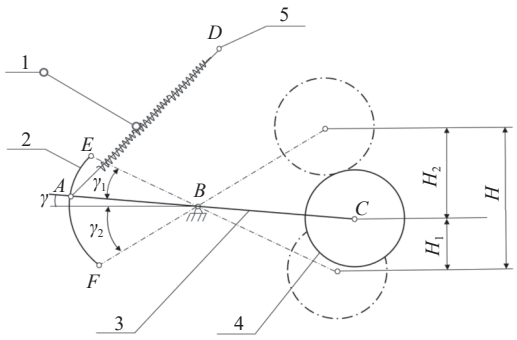

Note: L_{AC} is the length of the connecting plate, cm; L_{BC} is the distance from the hinge point to the compression wheel, cm; Point A is the traction point when the horizontal position of the ditch compression device, Point B is the hinge point of the connecting plate and the fixed frame, Point C is the center of the beating wheel, Point D is the fixed position of the connecting bolt, Point E is the upper profiling insertion point, F is the lower profiling insertion point, H is the total profiling amount, cm; H_1 is the lower profiling amount, cm; H_2 is the upper profiling amount, cm; γ is the traction angle during work, (°); γ_1 is the lower profiling angle, (°); $\gamma+\gamma_2$ is the upper profiling angle, (°).

Figure 7 Schematic diagram of the profiling structure

The lower affine quantity H_1 can be found from the graph:

$$H_1 = L_{BC}\sin(\gamma+\gamma_1) - L_{BC}\sin\gamma \tag{15}$$

The upper affine H_2:

$$H_2 = L_{BC}\sin\gamma + L_{BC}\sin\gamma_2 \tag{16}$$

The total affine volume H:

$$H = H_2 + H_1 = L_{BC}\sin(\gamma+\gamma_1) + L_{BC}\sin\gamma_2 \tag{17}$$

The amount of profiling is determined by the length of L_{BC} and the angle of profiling together. In the Huang-Huaihai region, wheat is usually ploughed twice before sowing, and the soil is relatively soft and flat, so the requirement for the profiling volume is not high, and the total profiling depth is usually about 10 cm[28]. To make the profiling mechanism work stably, the profiling angle should be reduced the better to meet actual demand. The length of the connecting rod L_{BC} can be lengthened to increase the profiling volume, however, if L_{BC} is too long, the center of gravity will be shifted back and the structure will not be compact. Here, point B was taken in the middle of AC, the length of the connecting rod AC is 16 cm, then L_{BC} = 8 cm. The traction angle γ is 0°, γ_1 is 30°, γ_2 is 40°. Then the upper profiling volume is 5.14 cm, the lower profiling height is 4 cm, and the total profiling depth is 9.14 cm.

3.2.3 Determination of tensile spring parameters

Figure 8 is the pressure mechanism load diagram. Considering the connecting plate and the press roller en bloc, the force generated between them is regarded as the internal force of the system. The overall mechanism is subjected to the tension in the spring to the connecting member as F_k, N; and the force of the ground to the press roller as F_0, N; γ is the traction angle, (0°); that is, the connecting rod is horizontal; α is the angle between the spring tension and the horizontal plane, taken as 60°.

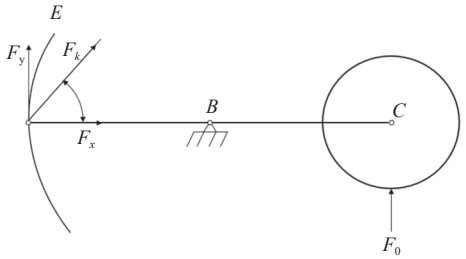

Note: F_k is the spring tension force, N, F_x, F_y are the horizontal and vertical component of the spring tension force, N; F_0 is the ground force on the pressure wheel, N; α is the angle between the spring tension force and the horizontal plane, (°).

Figure 8 Pressure mechanism load diagram

The press roller will apply a load Q_x to the ground and $F_0 = Q$. The balancing equation for the ballast mechanism is invoked to find the load Q_x.

$$\sum M_B = 0,\ F_0 L_{BC}\cos(\gamma) + F_k L_{AC}\sin(\gamma) - F_k\sin(\alpha)L_{AC}\cos(\gamma) = 0 \tag{18}$$

$$Q_x = F_0 = 0.866F_k \tag{19}$$

When the press roller is compressed, the seed trench is subjected to wheel load and gravity, and the calculation of the seed trench sinkage can be simplified as

$$Z_O = \frac{6Q_x}{5KB_0D_3^{\frac{1}{2}}} \tag{20}$$

$$K_x = \alpha_0(1+0.27B_0) \tag{21}$$

where, Z_0 is the amount of soil subsidence, cm; B_0 is the width of the press roller, cm; Q_x is the load on the press roller, N; D_3 is the diameter of the press roller, cm; K_x is the soil characteristic coefficient; α_0 is the parameter related to soil properties.

The ground area S_1, cm^2; of the press roller is

$$S_1 = B_0L_0 = \frac{B_0\beta D_3}{2} \tag{22}$$

$$\cos\beta = \frac{(D_3-2Z_0)}{D_3} \tag{23}$$

where, β is the contact angle between the press roller and the ground after sinking (°); L_0 is the arc length of contact between the press roller and the ground, cm. D_3 refers to the diameter of the ballast (in theory), cm. The ballast strength P is generally between 30 and 50 kPa[29].

$$P = \frac{Q_x}{S_1} \tag{24}$$

Combining Equations (16)-(22):

$$30 \le \frac{1732F_k}{BD_3\arccos\left(\frac{D_3-2Z_0}{D_3}\right)} \le 50 \tag{25}$$

The diameter of the press roller affects the compression delivered: the larger the diameter, the longer the compression time, the better the compression effect, and the smaller the slip rate. The diameter of the press roller for crops is 20-50 cm (herein, the diameter of the press roller D_3 is set to 23 cm). The width of the seed trench is 8 cm, the width of the press roller should be less than this (the width of the press roller B_0 is set to 7 cm). The press roller was made of tyre rubber, thereby reducing the slip rate.

The press roller compressed the soil in the open seed trench and a small part of the backflow of loose soil, the sink value Z_0 is determined in-situ to take the soil in the soil tank box to simulate the field wheat open trench compression environment. When the compression strength reaches around 40 kPa, the amount of soil sink is measured several times, and the average value of 1.8 cm is substituted into Equation (23) to obtain $155 \le F_k \le 259$ (N);

$$F_k = k\Delta x \tag{26}$$

where, k is the spring stiffness, N/m; Δx is the deformation, m. The requirement for the spring is a certain preload, and the spring is at point E with just stretched. The length of the spring when working is L_{AD}:

$$L_{AD} = \frac{L_{AB}}{\cos\alpha} \tag{27}$$

Here, L_{AD} =16 cm; The length of the DE segment L_{DE} = 8 cm, so, in the working state Δx= 8 cm, that is, $1.94 \le k \le 3.24$. For the sown soil in the Huang-Huaihai region, the soil is relatively soft, the ballast strength was taken to be 40 kPa, and the required F_k value is 207 N.

In the literature[30] the parameters of the cylindrical extension spring were selected as the middle diameter of 1.2 cm; the number of turns is 35; and the diameter is 0.2 cm: the spring stiffness factor k = 0.264 N/cm.

4 Discrete element simulation of key components

4.1 EDEM simulation parameter setting

The EDEM discrete element simulation software was used to simulate the key parameters of the homogeneous soil compression roller. The particle contact model, Hertz-Mindlin with bonding was chosen to simulate the contact action of conventional particles. Combined with existing studies[31-33], the model parameters of the seed trench compression device and soil as well as the contact parameters are listed in Table 3.

Table 3 Parameter selection in discrete element simulation analysis

Parameters	Values
Particle poisson's ratio	0.26
Particle shear modulus/MPa	20
Particle density/kg·m^{-3}	1300
Soil normal modulus/N·m^{-2}	2.3e+06
Soil tangential modulus/N·m^{-2}	1.6e+06
Soil normal stress/N	50 000
Soil tangential stress/N	25 000
Soil bond radius/mm	3.2
Soil particle radius/mm	3
steel Poisson's ratio	0.26
steel shear modulus/MPa	7.9e+04
steel density/kg·m^{-3}	7865
P-P restitution	0.14
P-P static friction	0.56
P-P rolling friction	0.3
P-S restitution	0.2
P-S static friction	0.6

4.2 Determination of key parameters of screed ballast roller

To determine the best combination parameters of the pre-sowing compression device, the height of the spiral blade h_0, the distance L_a between the spiral blade and the outermost end of the rut, and the rotational speed n, were selected as factors, and the soil flatness after operation was used as an evaluation index. An orthogonal combination test was conducted.

The EDEM model of the soil trough containing the ruts was built and imported into the SolidWorks model of the screed ballast roller for simulation (simulation parameters are listed in Table 3). The overall soil trough is a rectangular body of 200 cm in length, 180 cm in width, and 10 cm in height, and the middle recessed part is a simplified tractor rut. A forward roller motion with a tractor maintaining the same speed of 1.67 m/s was designed, according to actual measurements: the spiral blade in the soil will undergo a settlement of 1 cm, the blade is inserted into the soil to a depth of about 1 cm: the simulation incorporated this factor to establish, as shown in Figure 9, a homogeneous soil ballast roller-soil simulation model.

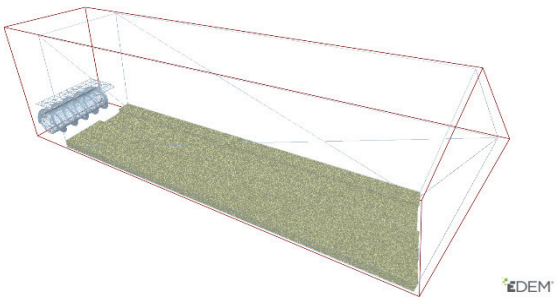

Figure 9 Simulation diagram of homogenization roller

4.3 Response surface experimental design

According to the previous design calculation, the height of the screed compression roller spiral blade is 9 cm≥ h_0 ≥ 3 cm, according to Equation (3), the greater the height of the spiral blade the more

the amount of screed. The distance between the spiral blade and the outermost end of the rut is 40 cm≥ L_a ≥ 0 m. The rotational speed n is such that 337.5 r/min ≥ n ≥ 88 r/min. According to Equation (3), the higher the angular velocity, the greater the amount of soil levelling. However, the influences of the above three factors on the soil on the levelling X are unclear: to explore their interaction and determine the best design and operation parameters of the screed ballast roller, the interaction test was designed. The table of test factor levels is listed in Table 4.

Table 4 Interactive test factor level table

Levels	Height of spiral blade h_0/cm	Range L_0/cm	Rotational speed n/r·min^{-1}
1	3	0	88
2	6	20	212.75
3	9	40	337.5

Soil flatness calculation method referred to Reference [28]. Taking the highest point of distance from the surface to the baseline was measured after ploughing; five such sections were selected, and the mean and standard deviation calculated according to Equations (28) and (29): the soil level and evenness are expressed as the value of standard deviation (the more level the soil the lower its standard deviation).

$$\alpha_j = \frac{\sum_{i=1}^{n_j} \alpha_{ji}}{n_j} \tag{28}$$

$$S_j = \sqrt{\frac{\sum_{i=1}^{n_j} (\alpha_{ji} - \alpha_j)^2}{n_j -}} \tag{29}$$

where, α_j denotes the average value of soil levelling in j^{th} trip, cm; α_{ji} denotes the measured value of soil levelling at i^{th} test point in j^{th} trip, cm; n_j is the number of test points in j^{th} trip; S_j denotes the standard deviation of soil levelling in j^{th} trip[34], cm.

4.3.1 Response surface test results analysis

Using Design-Expert software, Box-Behnken response surface tests were conducted with five center-points and a total of 17 tests, and the test protocols and their results are listed in Table 5.

Table 5 Schemes and results of response surface test

No.	Height of spiral blade h_0/cm	Range L_0/cm	Rotational speed n/r·min^{-1}	The surface roughness of soil/cm
1	3	0	212.75	0.25
2	9	0	212.75	0.35
3	3	40	212.75	0.26
4	9	40	212.75	0.31
5	3	20	88	0.26
6	9	20	88	0.29
7	3	20	337.5	0.27
8	9	20	337.5	0.38
9	6	0	88	0.25
10	6	40	88	0.2
11	6	0	337.5	0.29
12	6	40	337.5	0.31
13	6	20	212.75	0.19
14	6	20	212.75	0.2
15	6	20	212.75	0.21
16	6	20	212.75	0.21
17	6	20	212.75	0.19

The software was used to process the experimental results, and the regression model of soil levelling X was established separately using the modified model, and significance analysis was conducted using the regression model (Table 6). As can be seen from Table 6, the p value of the regression model of X is less than 0.0001, and the p value of the out-of-fit term is greater than 0.05, which indicates that the regression provides a better fir. Each factor has a significant effect on X. The regression equation is given by Equation (30)[24].

$$X = 0.2000 + 0.0362A - 0.0075B + 0.0313C - 0.0125AB + 0.0200AC + 0.0175BC + 0.0650A^2 + 0.0275B^2 + 0.0350C^2 \tag{30}$$

Table 6 Variance analysis of regression model

Source	Sum of Squares	df	F-value	p-value
Model	5.0×10^{-2}	9	54.58	< 0.0001**
A	1.0×10^{-2}	1	101.5	< 0.0001**
B	4.0×10^{-4}	1	4.34	0.0756
C	7.8×10^{-3}	1	75.43	< 0.0001**
AB	6.0×10^{-4}	1	6.03	0.0437*
AC	1.6×10^{-3}	1	15.45	0.0057**
BC	1.2×10^{-3}	1	11.83	0.0109**
A^2	1.7×10^{-2}	1	171.76	< 0.0001**
B^2	3.2×10^{-3}	1	30.74	0.0009**
C^2	5.2×10^{-3}	1	49.8	0.0002**
Residual	7.0×10^{-4}	7		
Lack of Fit	3.0×10^{-4}	3	1.08	0.4515
Pure Error	4×10^{-4}	4		
Total	0.0516	16		
R^2	0.9859			

Note:* shows this term is significant (p<0.05);** shows this term is very significant (p<0.01). The same below.

According to the regression model ANOVA table, the spiral blade height A interacts with rutting distance B, spiral blade height A with rotational speed C, and rutting distance B with rotational speed C. The pattern of the two sets of interaction factors on X was analyzed according to the generated response surface plots. Response surface diagrams of each factor interaction to working resistance is shown in Figure 10. It can be found that with the increases of the three factors, the soil levelling X tends to decrease first and then increase, indicating that when the moderate spiral blade height, rutting distance, and rotational speed were taken, the soil disturbance is the smallest and the soil return effect is the best, while when the individual factors are assigned smaller or larger values, the soil levelling X will increase and the levelling becomes worse due to too little soil return or excessive soil movement.

4.3.2 Optimal combination of screed ballast roller parameters

The smaller the value of soil levelling X, the better the effect. Using the Optimization-Numerical module in Design-Expert, the minimum value of soil levelling X is set as the target to solve the optimal combination of soil levelling roller parameters. The result of the simulation is shown in Figure 11. The result is X = 0.18, giving the lowest soil levelling value and the best effect.

5 Field trials

5.1 Test conditions and test methods

5.1.1 Test conditions

The experiment was conducted from October 24-25, 2021 at the Yuanyang base of Henan Agricultural University, Xinxiang, Henan Province, China. A double compression seeder for pre-sowing and seed furrow of wheat in wide-seedling belts was

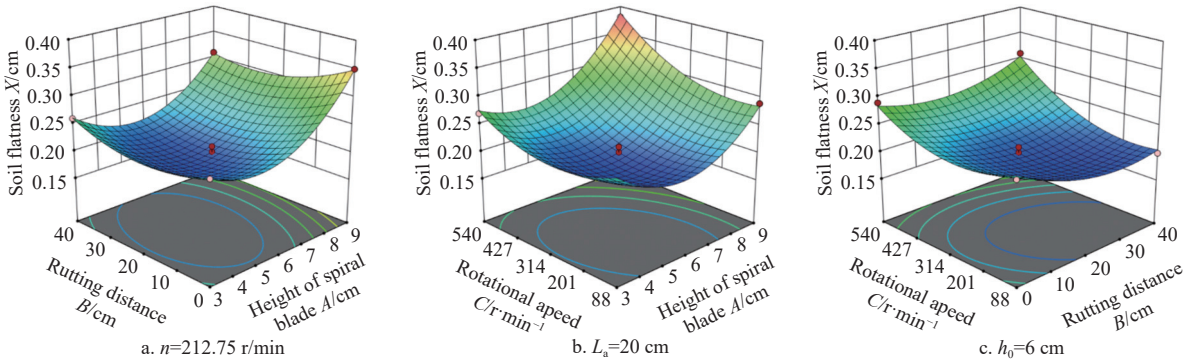

Figure 10 Response surface diagrams of each factor interaction to working resistance

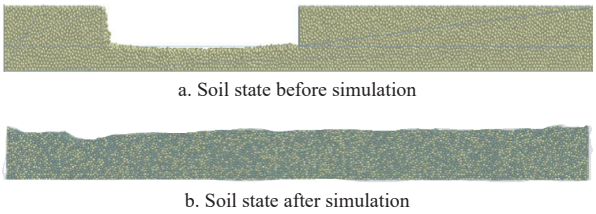

a. Soil state before simulation

b. Soil state after simulation

Figure 11 Simulation effect picture

compared with the common models sold in the market (use of the compression method entails compaction of top soil after sowing) in a series of sowing tests. The test field had a moisture content of 12%, a soil firmness of 130 kPa from 0-5 cm, 255 kPa from 5-10 cm, 385 kPa beyond 10 cm, and a capacity of 0.97 g/cm³ from 0-20 cm. The previous crop was corn and the wheat variety was Xinmai 26 with a thousand-grain weight of 40 g. The seeding rate was set to 195 kg/hm². The seeding depth was 3-5 cm. The test equipment included a ring knife, a TJSD-750-IV soil compactness meter, a steel ruler, a WYS-1 soil moisture meter, an oven, and an electronic scale. The test site is illustrated in Figure 12.

Figure 12 Field test

5.1.2 Test method

To verify the operational performance of the double compression seeder for pre-sowing and seed furrow of wheat in wide-seedling belts, the soil bulk density of the seed bed, the coefficient of variations in the sowing depth, soil firmness and seedling emergence were used as test indicators. The test method refers to the national and industry standards such as "NY/T 1143-2006 Technical Specification for Seeder Quality Evaluation" and "GB/T 9478-2005 Test Methods for Grain Strip Sowers".

1) Soil bulk density

The ring-knife method was used to measure soil volume over depths from 0-20 cm. The inner diameter of the ring knife r was 5 cm and the height was 6.37 cm. the volume was 0.5 L.

Calculation of the soil bulk density:

$$\rho = \frac{m}{V} = \frac{m}{\pi r^2 h} \tag{31}$$

where, ρ is the soil bulk weight, g/cm³; m is the mass of soil inside the ring knife after drying, g; V denotes the volume of soil inside the ring knife, cm³; r is the inner diameter of the ring knife, cm; h is the height of soil inside the ring knife, cm.

2) Coefficient of variation of the seeding depth

After the tractor sows seeds at normal operating speed, 6 rows are randomly taken, and each row is randomly selected 10 points (giving a line of measurement points) within 50 m to measure its depth. The design mulching depth was taken as the middle value of 4 cm.

The coefficient of variations (CV) in the sowing depth is calculated as

$$CV = \frac{S_2}{\bar{x}} \times 100\% \tag{32}$$

where, S_2 is the standard deviation of seed depth; $\bar{x}$ is the mean depth to a seed.

3) Soil compactness measurement

Five random rows of seeding rows were taken from the test plots after the operation of both seeders, and five points were randomly taken from each row to measure the soil firmness of the 0-5 cm, 5-10 cm and 10-15 cm soil layers, and the average value was taken.

4) Soil levelling measurement

Soil flatness is an important factor affecting the quality of sowing, and a flat soil is more conducive to maintaining a consistent sowing depth. Soil levelness is calculated by referring to the literature.

5) Emergence status

Seedling height is an important trait of wheat seedlings and reflects the growth of seedlings[35,36]. On the tenth day after wheat sowing, when wheat seeds had emerged and were of a certain length, intact wheat plants were randomly removed and rinsed for comparison in the pre-sowing and seed furrow double compression seeder and common seeder sowing areas in the wide-seedling belt wheat to measure seedling length and count the number of primordial roots.

5.2 Experimental results and analysis

The results of the soil bulk density tests before and after sowing with the double compression seeder for pre-sowing and seed furrow of wheat in wide-seedling belts are listed in Table 7.

Table 7 Results of soil bulk density test before and after sowing

	Sample No.						Average value
	1	2	3	4	5	6	
Soil before sowing/g·cm⁻³	0.89	1.02	0.96	0.89	0.95	1.06	0.97
Soils after sowing/g·cm⁻³	1.22	1.16	1.24	1.31	1.08	1.16	1.19

As can be seen from Table 7, the average soil bulk density of wheat before sowing was 0.97 g/cm^3, and the average soil bulk density of wheat after sowing was 1.19 g/cm^3, which was 22.7% (p < 0.01) greater than that before sowing. This proves that the compression roller of the pre-sowing compression device compacted the loose pre-sowing soil to some extent, which reduced the gaps between the soil peds and improved the compactness of the sown soil and decreased the evaporation of soil moisture.

The results of the comparison test between the double ballast seeder and the common seeder before sowing and seed furrow of wheat in wide seedling belts are listed in Table 8.

As can be seen from Table 8, the average sowing depth of the double compression seeder for pre-sowing and seed furrow of wheat in wide-seedling belts is 3.94 cm with a coefficient of variation of 8.8%, while the average sowing depth of a common seeder is 3.86 cm with a coefficient of variation of 14.2%. This is because the press roller flattens the seeds and the protruding soil and loose soil in the seed furrow after the seeds fall into the seed furrow, and the shape of the seed furrow is more stable and flat; at the same time, it also makes the seeds set firmly on the soil surface of the seed furrow, which increases the stability of the seeding depth of the seeder.

Table 8 Comparison test results of seeder

Type of seeder	Sowing depth		Average soil firmness/kPa			Seedling length	Soil bulk density	The surface roughness of soil
	Average value/ cm	Coefficient of variation/%	0-5 cm	5-10 cm	10-15 cm	Average value/ cm	Average value/(g·cm^{-3})	Average value/cm
Double pressure seeder for wheat before sowing and seed groove	3.94	8.88	15.04	30.38	41.07	15.49	1.19	1.9
Ordinary seeder	3.86	14.16	18.05	26.07	39.90	13.23	1.10	2.9

In the soil layer from 0-5 cm, the soil firmness of the common seeder was 30 kPa greater than that of the double compression seeder for pre-sowing and seed furrow of wheat in wide-seedling belts, which was because the common seeder was suppressing the surface layer of the soil and compacting the surface soil, while the double compression seeder for pre-sowing and seed furrow of wheat in wide-seedling belts did not compact the surface soil; from 5-10 cm the soil firmness of the double compression seeder for pre-sowing and seed furrow of wheat in wide-seedling belts was 43 kPa greater than that elsewhere: this indicates that the soil firmness from 5-10 cm in the soil is significantly changed by the use of seed trench compression; the difference between the soil firmness in the soil layer from 10-15 cm is 12 kPa, and with the increase in depth, the soil firmness of the seed trench compression and the unsuppressed soil layer tends to be the same; in summary, after the seeds are compacted by seed trench compression at a depth of 3-5 cm, the soil below the seeds is also compacted. The soil below the seeds was also compacted and the top of the seeds was covered with loose soil. Compared with mulching, seed trench compression creates a solid environment for the seeds to grow, with the loose soil above helping to absorb oxygen and the compact soil below helping the seeds to absorb water from it, which is more in line with agronomic requirements.

The wheat preplant and seed furrow double ballast seeder increased the capacity by 8.12% compared with the common seeder. Soil levelling was improved from 2.9 cm to 1.9 cm, indicating that the front ballast levelling roller played a beneficial role in soil levelling (compared with the simulation results, the error was 5.26%, suggesting the simulation results were reliable).

On the tenth day after sowing, the wheat seedling length of the broad strip wheat pre-sowing and seed trench double compression seeder was 17.1% longer than that of the ordinary seeding suppressor, and the seedling emergence of the seed trench compression was significantly better than that of the seed trench unsuppressed, which was because the wheat sowing depth was more stable after seed trench compression, and the soil under the seed was tight and consistent, which was more conducive to the seed absorbing water as it seeps downwards, while the soil above the seed was loose and the seed was more easily exposed thereto. At the same time, the soil above the seeds is loosened and the seeds are more readily exposed to oxygen, which is conducive to seed germination and the growth of seedlings.

Comprehensive field comparison tests show that the method of sowing with double compression before sowing and in the seed furrow can improve the soil environment of the seed bed, enhance the compactness of the soil in the seed furrow, improve soil levelling, increase the soil bulk density, and improve the uniformity of the sowing depth.

6 Conclusions

1) The double compression seeder for pre-sowing and seed furrow of wheat in wide-seedling belts designed mainly completes the pre-sowing compression and seed furrow compression processes: pre-sowing compression adopts an equal-difference variable pitch spiral winch blade and compression drum for pre-sowing after wheel traffic (and the concomitant soil compression); after the seed drops, use the seed furrow compression device to depress the seed and soil in the seed furrow, so that the seed is embedded in the soil within the furrow. Finally, the seeding operation is completed by mulching the soil on the surface of the seed furrow with the mulcher;

2) The structure design and parameters of the pre-planting compression device and the seed furrow compression device were determined. The pre-sowing compression device was simulated by EDEM software, and the isotropic variable diameter and equal pitch spiral conveying strand was selected with a drum diameter of 30 cm, a starting spiral blade diameter of 6 cm, an ending spiral blade diameter of 5.5 m, a pitch of 4.8 m, and an angular velocity of 327 r/min. The diameter of the press roller of the seed furrow compression mechanism is 23 cm and its width is 7 cm. The spring stiffness factor K is 0.264 N/cm. The relative error between the simulation results of the pre-sowing compression roller and the field test results is 5.26%, suggesting that the simulation is reliable;

3) The results of the field comparison test with the common seeder show that the soil bulk density after the operation of the double compression seeder for pre-sowing and seed furrow of wheat in wide-seedling belts increased by 22.7% after sowing compared with that before sowing (p<0.01); the coefficient of variation of the sowing depth of the double compression seeder for pre-sowing and seed furrow of wheat in wide-seedling belts decreased by 37.9% compared with that of the common seeder (p<0.01), and the soil firmness increased by 43.04% from 5 to 10 cm deep with an 8.12%

increase in bulk unit weight. The wheat seedling length on the 10th day after sowing was 17.1% greater than that of the ordinary seeder. The proposed machinery improved the soil environment in and around the seed bed, increased the uniformity of the sowing depth, and promoted the growth and development of wheat. It provides equipment support and a technical reference for wheat-corn rotation areas in the Huang-Huaihai region of China.

Acknowledgements

This research was financially supported by Henan Province Science and Technology Project (Grant No. 232102110271) and China Agriculture Research System (Grant No. CARS-03-44).

[References]

[1] Zhou J H, Wang J Y, Meng F Y, Tong G X, Mei L, Liu G M, et al. Effects of tillage methods on sowing quality, yield and benefit of wheat. Crops, 2022; 4: 19–204. (in Chinese)

[2] Xu Q M, Li H W, He J, Wang Q J, Lu C Y, Wang C L. Design and experiment of the self-propelled agricultural mobile platform for wheat seeding. Transactions of the CSAE, 2021; 37(14): 1–11. (in Chinese)

[3] Liu J Y, Cui Z K, Ma J C, Jiao W. Problems and countermeasures of wheat corn rotation production mechanization for main crops in Huanghuaihai Region. Journal of Agricultural Mechanization Research, 2016; 38(5): 259–263. (in Chinese)

[4] Wang X L, Wang Q J, Li H W, li W, Niu Q, Chen W Z. Effect of tyre induced soil compaction on soil properties and crop root growth under no-tillage system. Transactions of the CSAM, 2017; 48(6): 168–175. (in Chinese)

[5] Nielsen S K, Munkholm L J, Lamandé M, Michael N, Edwards G T C, Green O. Seed drill depth control system for precision seeding. Computers and Electronics in Agriculture, 2018; 144: 174–180.

[6] Zhang X Y, Sui Y Y. Summarization on the effect of soil compaction on crops. Transactions of the CSAM, 2005; 36(10): 161–164. (in Chinese)

[7] Luo H Q, Liu X, Qin J T, Zhao J W. Study on the compacting device of combination for ridge-till and no-till planters. IOP Conference Series: Materials Science and Engineering. IOP Publishing, 2019; 638(1): 012017.

[8] Pinheiro V, Stone L F, Barrigossi J A F. Rice grain yield as affected by subsoiling, compaction on sowing furrow and seed treatment. Revista Brasileira de Engenharia Agrícola e Ambiental, 2016; 20: 395–400.

[9] Luo W W, Gu F W, Wu F, Xu H B, Chen Y Q, Hu Z C. Design and experiment of wheat planter with straw crushing and inter-furrow collecting-mulching under full amount of straw and root stubble cropland. Transactions of the CSAM, 2019; 50(12): 42–52. (in Chinese)

[10] Zhang R T, Ma C Y, Ma J H, Liu J. Difference analysis of the effects of different suppression methods on winter wheat yield. Agriculture and Technology, 2021; 41(1): 22–24. (in Chinese)

[11] Patel S K, Mani I, Sundaram P K. Effect of subsoil compaction on rooting behavior and yields of wheat. Journal of Terramechanics, 2020; 92: 43–50.

[12] Jourgholami M. Effects of soil compaction on growth variables in Cappadocian maple (Acer cappadocicum) seedlings. Journal of Forestry Research, 2018; 29(3): 601–610.

[13] Wahlstrom E M, Kristensen H L, Thomsen I K, Labouriau R, Pulido-Moncada M, Nielsen J A, et al. Subsoil compaction effect on spatio-temporal root growth, reuse of biopores and crop yield of spring barley. European Journal of Agronomy, 2021; 123: 126225.

[14] Bronick C J, Lal R. Soil structure and management: A review. Geoderma, 2005; 124(1-2): 3–22.

[15] Liu Q T, Zhang J G, Yang N, Zhao X K, Wang H, Zhao J, et al. Study on the pulverizer repression wheel before sowing of the precise planter with no-tillage subsoil and whole layer fertilization. Journal of Agricultural Mechanization Research, 2015; 37(7): 127–130. (in Chinese)

[16] Wei G J, Shi S, Zhou J L, Liu H, Zhang R F. Design and experiment of double press seeder with wide seedling belt of wheat. Shandong Agricultural Sciences, 2020; 52(10): 138–143. (in Chinese)

[17] Zhao S H, Tan H W, Wang J Y, Yang C, Yang Y Q. Design and experiment of multifunctional integrated seeding opener. Transactions of the CSAE, 2018; 34(11): 58–67. (in Chinese)

[18] Jia H L, Wang W J, Luo X F, Zheng J X, Guo M Z, Zhuang J. Effects of profiling elastic press roller on seedbed properties and soybean emergence under double row ridge cultivation. Soil & Tillage Research, 2016; 162: 34–40.

[19] Xi X B, Gua C J, Shi Y J, Zhao Y, Zhang Y F, Zhang Q, et al. Design and experiment of no-tube seeder for wheat sowing. Soil and Tillage Research, 2020; 204: 104724.

[20] Wang Q N. Calculation method of rolling resistance and sinkage when rigid wheels pass through loose soil for many times. Journal of Jilin University of Technology, 1987; 3: 53–62.

[21] Liu W R, Chen J, He H, Zhu C H, Wang W Z. The design and test of electric control system of wheat seeder. Journal of Agricultural Mechanization Research, 2021; 43(1): 46-51. (in Chinese)

[22] Liu K, Gao J D, Ma G Z, Wang B. Exploration and practice of soil mechanical subsoiling in high yield well irrigation area in Shandong Province. Agricultural Engineering, 2020; 10(7): 12–18. (in Chinese)

[23] Transportation Machinery Design Selection Manual Committee. Transportation Machinery Design Selection Manual. Beijing: Chemical Industry Press, 1999. (in Chinese)

[24] Yuan Q C, Xu L M, Niu C, Ma S, Yan C G, Zhao S J, et al. Development of soil-fertilizer mixing layered backfiller for organic fertilizer deep applicator in orchard. Transactions of the CSAE, 2021; 37(5): 11–19. (in Chinese)

[25] Zheng K, Liu G Y, Guo L W, Cheng J, Xia J F, Li Y F. Design and experiment of wide-boundary seldom-tillage wheat planter with soil-shunting function. Transactions of the CSAM, 2022; 53(2): 128–138. (in Chinese)

[26] Jia H L, Meng F H, Liu L J, Shi S, Zhao J L, Zhuang J. Biomimetic design and experiment of core-share furrow opener. Transactions of the CSAM, 2020; 51(4): 44–49, 77. (in Chinese)

[27] Aikins K A, Jensen T A, Antille D L, Barr J, Ucgul M, Desbiolles J. Evaluation of bentleg and straight narrow point openers in cohesive soil. Soil and Tillage Research, 2021; 211: 105004.

[28] Zhao S H, Jiang E C, Yan Y X, Yang Y Q, Tian B L. Design and motion simulation of opener with bidirectional parallelogram linkage profiling mechanism on wheat seeder. Transactions of the CSAE, 2013; 29(14): 26–32. (in Chinese)

[29] Lu Q, Wang L, Liu Y, Li L H, Liu L J, Zheng D C. Effects of different suppression intensity on growth characteristics of oat. Agricultural Engineering, 2022; 12(7): 88–94. (in Chinese)

[30] Wang W B, Lin Z Q. Mechanical design manual. Beijing: Mechanical Industry Press, 2004.

[31] Ma S, Xu L M, Yuan Q C, Niu C, Zeng J, Chen C, et al. Calibration of discrete element simulation parameters of grapevine antifreezing soil and its interaction with soil-cleaning components. Transactions of the CSAE, 2020; 36(1): 40–49. (in Chinese)

[32] Liu R, Li Y J, Liu C X, Liu L J. Design and experiment of shovel type wide seedling belt oat seeding furrow opener. Transactions of the CSAM, 2021; 52(9): 89–96. (in Chinese)

[33] Guo C C, Li G H, Zhang J C, Jin X N, Xue J F, He C X, et al. Influence of the sweep angle of the cross knife opener on soil disturbance. Inmateh-Agricultural Engineering, 2020; 62(3): 317–324.

[34] Li C F, Li K, Lei C J, Li G H, Zhang D L, He X W. Experimental analysis on working performance of jz01-4800 combined soil preparation machine. Agricultural Mechanization Research, 2018; 40(10): 172–176. (in Chinese)

[35] Lazukin A V, Gundareva S V, Grabelnyh O I, Saidova L T, Dorofeev N V, Romanov G A, et al. Effect of pre-sowing ozone treatment on low temperature tolerance in spring wheat (*Triticum aestivum*) seedlings. Research on Crops, 2021; 22(3): 478–482.

[36] Zang H C, Wang Y J, Zhang J, Li F, Lu H F, He D X. Difference analysis in morphological and physiological characteristics between seminal and nodal roots of winter wheat (*Triticum aestivum* L.). Journal of Henan Agricultural Sciences, 2018; 47(6): 18–23. (in Chinese)